Nuclear Science and Techniques (2023) 34:139
https://doi.org/10.1007/s41365-023-01285-1

Comparison between 4D robust optimization methods for carbon-ion treatment planning

Wen-Yu Wang[1,2,3,4] · Yuan-Yuan Ma[1,2,3,4] · Hui Zhang[1,2,3,4] · Xin-Yang Zhang[1,2,3,4] · Jing-Fen Yang[1,2,3,4] · Xin-Guo Liu[1,2,3,4] · Qiang Li[1,2,3,4,5]

Received: 14 February 2023 / Revised: 31 May 2023 / Accepted: 3 June 2023 / Published online: 23 September 2023

Abstract

Intensity-modulated particle therapy (IMPT) with carbon ions is comparatively susceptible to various uncertainties caused by breathing motion, including range, setup, and target positioning uncertainties. To determine relative biological effectiveness-weighted dose (RWD) distributions that are resilient to these uncertainties, the reference phase-based four-dimensional (4D) robust optimization (RP-4DRO) and each phase-based 4D robust optimization (EP-4DRO) method in carbon-ion IMPT treatment planning were evaluated and compared. Based on RWD distributions, 4DRO methods were compared with 4D conventional optimization using planning target volume (PTV) margins (PTV-based optimization) to assess the effectiveness of the robust optimization methods. Carbon-ion IMPT treatment planning was conducted in a cohort of five lung cancer patients. The results indicated that the EP-4DRO method provided better robustness ($P = 0.080$) and improved plan quality ($P = 0.225$) for the clinical target volume (CTV) in the individual respiratory phase when compared with the PTV-based optimization. Compared with the PTV-based optimization, the RP-4DRO method ensured the robustness ($P = 0.022$) of the dose distributions in the reference breathing phase, albeit with a slight sacrifice of the target coverage ($P = 0.450$). Both 4DRO methods successfully maintained the doses delivered to the organs at risk (OARs) below tolerable levels, which were lower than the doses in the PTV-based optimization ($P < 0.05$). Furthermore, the RP-4DRO method exhibited significantly superior performance when compared with the EP-4DRO method in enhancing overall OAR sparing in either the individual respiratory phase or reference respiratory phase ($P < 0.05$). In general, both 4DRO methods outperformed the PTV-based optimization in terms of OAR sparing and robustness.

Keywords Intensity-modulated particle therapy · Carbon-ion radiotherapy · Uncertainties · Four-dimensional robust optimization · Lung cancer · Relative biological effectiveness-weighted dose · Robustness · Treatment planning system

1 Introduction

Intensity-modulated particle therapy (IMPT) with carbon ions can deliver higher doses to the target volume while significantly sparing the adjacent organs at risk (OARs) [1, 2]. The sharp dose falloff behind the pristine Bragg peak of carbon-ion beams makes the dose distributions highly

This work was supported by National Key Research and Development Program of China (No. 2022YFC2401503), National Natural Science Foundation of China (Nos. 11875299, 61631001, U1532264, and 12005271).

✉ Qiang Li
liqiang@impcas.ac.cn

[1] Institute of Modern Physics, Chinese Academy of Sciences, Lanzhou 73000, China

[2] Key Laboratory of Heavy Ion Radiation Biology and Medicine of Chinese Academy of Science, Lanzhou 730000, China

[3] Gansu Provincial Key Laboratory of Basic Research on Heavy Ion Radiation Application in Medicine, Lanzhou 730000, China,

[4] University of Chinese Academy of Sciences, Beijing 100049, China

[5] Putian Lanhai Nuclear Medicine Research Center, Putian 351152, China

sensitive to uncertainties, which greatly diminishes the effectiveness of the IMPT [3]. Three of the most pertinent uncertainties in carbon-ion dose distributions include (1) the range uncertainty introduced by the uncertainty in computed tomography (CT) numbers and their conversion to relative stopping power [4]; (2) setup uncertainty is related to a lack of reproducibility in patient positioning [5]; (3) uncertainties introduced by respiratory motion, especially for patients with lung cancers [6]. The comparison of PTV-based optimization with robust optimization is a widely used approach for evaluating the robustness of treatment plans. Although the PTV concept has been employed in some studies of carbon-ion radiotherapy [7], it is insufficient for carbon-ion radiotherapy. Dose distributions are influenced by various factors, not only at the edges of the target volume but also inside the target volume [8].

To mitigate the impact of various uncertainties in carbon-ion IMPT, various three-dimensional robust optimization (3DRO) methods have been developed, including probabilistic optimization [9, 10], voxel-wise worst-case robust optimization [11], and worst-case scenario robust optimization [12]. These methods aim to incorporate uncertainties directly into optimization. Probabilistic methods optimize treatment plans based on a large number of dose distributions produced by a random sampling setup and range uncertainty scenarios with an assumed probability [3]. Voxel-wise worst-case robust optimization considers the minimum and maximum doses from all uncertainty scenarios for each voxel inside the target volume and maximum doses for each voxel inside the normal tissues. The worst-case dose distributions include the minimum and maximum doses. During the iterations, only one objective function based on the worst-case dose distributions was optimized. The worst-case scenario robust optimization method evaluates the objective function for all uncertainty scenarios and chooses the worst objective function score in the iteration process. Recent studies have shown that 3DRO methods can minimize the variance in dose distributions under different uncertainty scenarios and improve the robustness of treatment planning [13–17].

Target motion and motion-induced range changes play important roles in particle radiotherapy. The effectiveness of 3DRO methods in mitigating the effect of respiratory motion on lung cancer therapy is limited [18]. To explicitly account for respiratory motion in IMPT, different strategies have been proposed, mainly including respiratory gating and breath-holding. Unfortunately, these methods have limitations in terms of treatment time and patient tolerance requirements. Additionally, online motion tracking [19] is indispensable for moving targets in the treatment process to reduce the impact of breathing motion. However, this remains technically challenging. Another approach proposed by Graeff et al. [20] suggested that 4D optimization based on all motion states is valid for carbon-ion therapy. Liu et al. [21] introduced a reference phase-based 4D robust optimization (RP-4DRO) method, which optimizes cumulative 4D dose distributions. Ge et al. [3] proposed a method termed as phase-based 4D robust optimization (EP-4DRO), which optimizes dose distributions based on individual respiratory phase. Wolf et al. [7] proposed a robust nonlinear RBE-weighted optimization method to expand the carbon-ion IMPT, thus exploring the potential for improving plan robustness and sparing critical organs. These studies confirm that 4DRO methods can improve plan robustness and offer better control over uncertainties during treatment. However, there has been a persistent lack of comparative analyses among the different 4DRO methods in carbon-ion IMPT treatment planning, hindering a comprehensive understanding of the distinct characteristics of each method.

The relative biological effectiveness (RBE), which is defined as the ratio of a photon dose and an ion dose leading to the same biological effect under identical conditions [22], is widely used in particle therapy. A constant RBE value of 1.1 was clinically accepted for protons.

However, the RBEs of carbon ions must be described by mathematical models rather than by a single parameter because of their RBE values' sophisticated dependence on physical and biological factors. It is necessary to plan carbon-ion treatment with RBE-weighted doses (RWD), defined as the product of physically absorbed doses and RBE. Some models have been proposed, such as the mixed beam model, the local effect model (LEM), and the microdosimetric kinetic model (MKM) [22]. These models facilitate carbon-ion treatment planning using RWD.

An appropriate robust optimization method is crucial for addressing the dose perturbations arising from various uncertainties. To the best of our knowledge, no previous studies have compared the RP-4DRO and EP-4DRO methods. It is acknowledged that the RP-4DRO method does not explicitly optimize the dose distributions of the individual breathing phases. It is necessary to pay attention to the dose distributions in individual breathing phases for clinical implementation. To evaluate the effectiveness of 4DRO methods in carbon-ion IMPT, a comparative and analytical investigation of 4DRO methods is indispensable. The innovation is to compare and evaluate two theoretically different robust optimization methods in terms of RWD distributions in carbon-ion IMPT treatment planning.

2 Materials and methods

2.1 Treatment planning

MatRad [23], an open-source treatment planning system (TPS), was developed for educational and research purposes.

This also supports carbon-ion IMPT treatment planning. The energies of the carbon ions available in matRad are in the range of 115.23 MeV/u to 398.84 MeV/u corresponding to a penetration range of 32.68 mm to 294.25 mm in water. Furthermore, alpha-beta ratios of 10 and 2 were selected for the target volume and normal tissue, respectively. The dose grid was set to 3 mm × 3 mm × 3 mm in this study. The pencil beam scanning (PBS) method with spot scanning was used. Furthermore, PBS can realize conformal dose distributions for irregularly shaped tumors and improve the beam utilization [24].

Gaussian-shaped carbon-ion beam spot sizes range from 11.80 mm to 8.01 mm (full width at half maximum, FWHM) for energies in the range of 115.23 MeV/u to 398.84 MeV/u. A spot spacing of 3 mm in the lateral and longitudinal directions was employed. Carbon-ion IMPT treatment planning was performed in five patients with lung tumor lesions. For each patient, 4DCTs were acquired with 10 motion states. To reduce the consumption of computer memory, both 4DRO methods were developed using three significantly different breathing phases: 0% expiration phase, 80% expiration phase, and 40% inspiration phase. The 0% expiration phase was defined as the reference breathing phase.

For the PTV-based optimization, the PTV was generated by extending the union of the CTVs in all three phases with a 5-mm safety margin. The magnitude of the margins was derived from the original photon treatment planning [25]. The dose distributions were calculated for the three respiration phases without accounting for setup and range uncertainties. Both 4DRO methods were performed on the CTV for each phase without incorporating any margins. The setup uncertainties were assumed as ±5 mm in $\pm x$, $\pm y$, and $\pm z$ directions. The range of the uncertainty parameters was set to ±3.5% when the water-equivalent depth was computed. Each breathing phase had eight uncertain dose scenarios and one nominal dose scenario. The tumor size, location, magnitude of motion, and beam angle of the five patients under investigation are listed in Table 1. The CTV centroids in the right-left (RL), anterior-posterior (AP), and superior-inferior (SI) directions for the three breathing phases were recorded. The maximum centroid was used to determine the magnitude of the motion. The patient datasets included 4DCT images with CTV and OARs delineated by an experienced physician following the delineation guidelines provided in [26]. The prescription for all patients was 60 Gy (RBE)/15 fractions with threshold doses of 45, 20, and 30 Gy (RBE) for the spinal cord, lungs, and heart, respectively. The LEM was used to calculate RBE values.

Table 1 Tumor locations, volumes, and motion magnitudes of the patients under investigation

Patient ID	Tumor location	Tumor volume (cc)	Motion mag. (mm)	Beam angle(°)
1	Right hilar	47.23	20.0	220/140
2	Right hilar	56.99	19.0	220/140
3	Left hilar	40.86	12.0	210/140
4	Right lower	1.33	2.0	330/45
5	Right lower	64.31	5.0	330/45

2.2 4D robust optimization

Liu et al. [21] proposed a robust version of the 4D optimization method and demonstrated that this approach can enhance the robustness of the cumulative 4D dose distribution. The physical absorbed dose distributions ($d^s_{i_k,j}w^2_j$) in different setups and range uncertainty scenarios were calculated for the breathing phases of 4DCT datasets, where w_j represents the intensity weight of the beamlet j, and $d^s_{i_k,j}$ represents the influence matrix describing the distribution of the beamlet j in the breathing phase k to voxel i_k in the uncertainty scenarios. We define s as each uncertainty scenario considered during treatment planning optimization and define S as the set of all scenarios. During the optimization process, a nonnegative vector w^2_j was used to transform the constrained optimization problem ($w \geq 0$) into a non-constrained problem. The cumulative physically absorbed dose distributions were deformed to the reference breathing phase by using the registration algorithm in matRad. The cumulative RWD distributions D^s_i were computed using the cumulative physically absorbed dose distributions. Specifically, D^s_i were employed in a standard quadratic objective function to design a carbon-ion treatment plan. In the objective function, the worst-case scenario robust optimization mentioned above was conducted as follows:

$$\begin{aligned}\min f(w) = \sum_{N\in\text{Target}} \Big\{ & q_{n,\max} \max_{s\in S}(D^s_i - D_{\text{pre}})^2 \\ & + q_{n,\min} \min_{s\in S}(D^s_i - D_{\text{pre}})^2 \Big\} \\ & + \sum_{M\in\text{Oar}} q_{m,\max} \max_{s\in S} H(D^s_i - D_{\text{o}})(D^s_i - D_{\text{o}})^2,\end{aligned} \tag{1}$$

where D_{pre} and D_{o} denote the prescription dose in the target volume and dose constraints on the relevant tissues, respectively. Furthermore, N and M denote the numbers of target volumes and OARs, respectively. Parameters $q_{n,\max}$, $q_{n,\min}$, and $q_{m,\max}$ are the penalty factors for the target volumes and OARs. Furthermore, $q_{n,\max} = 1.0$, $q_{n,\min} = 1.0$, and $q_{m,\max} = 1.0$ were used. The step function H is mathematically defined as follows: $H = 1.0$ when $D^s_i > D_{\text{o}}$ and $H = 0.0$ otherwise. The ultimate objective of the optimization is to minimize the objective function $f(w)$ to realize the optimal dose distributions over the relevant voxels.

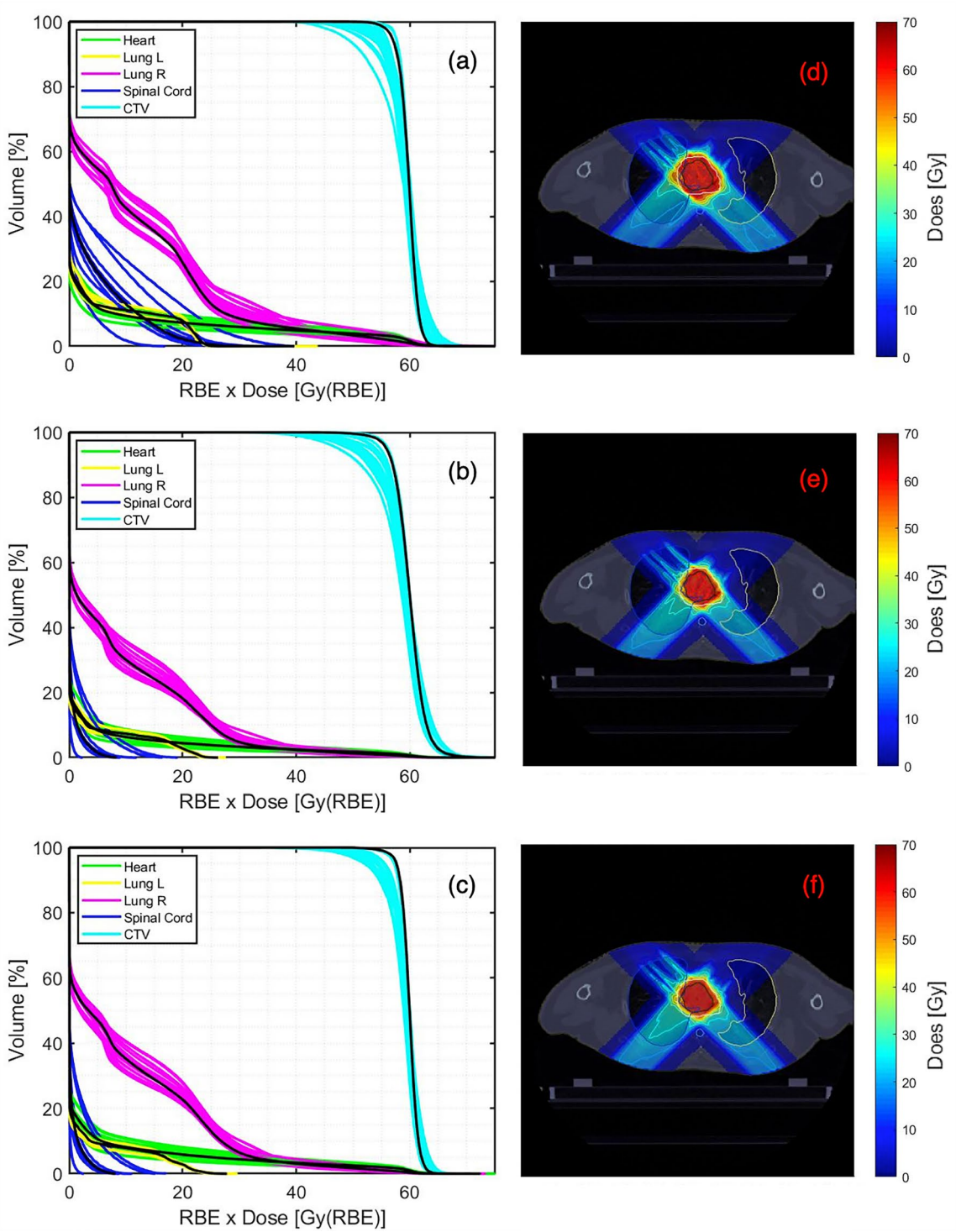

Fig. 1 (Color online) DVHs of Patient 1 for the different treatment plans using the PTV-based optimization (**a**), RP-4DRO (**b**), and EP-4DRO (**c**) methods. The axial view of the accumulated 4D dose distribution overlaid on the reference phase is displayed on panels (**d**–**f**), corresponding to the different plans

The RP-4DRO method did not explicitly address the optimization of dose distributions in the individual breathing phases; it remained unclear whether robustness in individual respiratory phases can be ensured. Ge et al. [3] proposed the EP-4DRO method for solving the uncertainty problem in proton treatment planning. The RWD

distributions $D^s_{i_k}$ in different setups and range uncertainty scenarios were calculated for all the breathing phases of 4DCT. The worst dose distributions for each breathing phase were calculated by selecting the worst objective score. Subsequently, the worst dose distributions for all the phases were simultaneously optimized. The objective function is expressed as follows:

$$\begin{aligned}\min f(w) = \sum_{N\in\text{Target}} \Bigg\{ \sum_{k\in K} q_{n,\max} \max_{s\in S}(D^s_{i_k} - D_{\text{pre}})^2 \\ + \sum_{k\in K} q_{n,\min} \min_{s\in S}(D^s_{i_k} - D_{\text{pre}})^2 \Bigg\} + \\ \sum_{M\in \text{Oar}} \sum_{k\in K} q_{m,\max} \max_{s\in S} H(D^s_{i_k} - D_{\text{o}})(D^s_{i_k} - D_{\text{o}})^2.\end{aligned} \tag{2}$$

It should be noted that all the parameter settings were the same as those in the RP-4DRO method. During the optimization iteration, the objective function values for each dose scenario were calculated, and the worst scenario was selected.

2.3 Plan evaluation

To maintain consistency, the resulting dose distributions for the volume of interests (VOIs) were evaluated and compared using the same parameters. Nine dose distributions for each breathing phase (6 setup uncertainty scenarios, 2 range uncertainty scenarios, and 1 nominal scenario) were calculated. The bands of dose-volume histograms (DVHs) derived from the 27 dose distributions (nine scenarios for three breathing phases) were analyzed to compare the robustness of the treatment plans. For PTV-based optimization, the dose distributions were recalculated for each breathing phase using the optimized set of spot intensities for each of the nine uncertainty scenarios. A narrower band in the DVH indicates greater robustness, implying that the dose distribution changes are relatively minimal under the influence of uncertainties. Evaluating DVHs with nine accumulated dose distributions is essential [3]. Thus, DVHs derived from the 9 accumulated dose distributions were also analyzed. Dose accumulation was assessed during the three breathing phases.

Dose distribution conformity index (CI) and target heterogeneity index (HI) were computed using the following equations:

$$CI = \frac{TV_{95\%}}{TV} \times \frac{TV_{95\%}}{V_{95\%}} \quad , \tag{3}$$

$$HI = \frac{D_{5\%} - D_{95\%}}{D_{95\%}} \quad . \tag{4}$$

Specifically, $TV_{95\%}$ denotes the target volume receiving a 95% prescription dose. Furthermore, $V_{95\%}$ represents the total volume receiving at least 95% of the prescribed dose; CTV is the target volume (TV) for the three methods. The CI is a measure of how well the target dose distributions conform to the target volume, with a value closer to 1.0 indicating greater conformity. HI reflects the homogeneity of the target dose distributions, with a value closer to 0.0 indicating greater homogeneity. To compare the target coverage, the index $D_{95\%}$ is used to represent the dose received by the 95% target volume. A value closer to the prescribed dose indicates better TV dose coverage of the target volume.

Normal tissue sparing was evaluated by comparing different treatment plans optimized using different methods. Evaluation indexes, such as lung D_{mean}, lung $V20$, lung $V5$, heart D_{mean}, heart $V30$, and spinal cord $D_{\max}$ were analyzed and compared among the aforementioned methods. Given that the dose distributions were non-Gaussian profiles, a statistical analysis was conducted using the Wilcoxon signed-rank test [27] to compare the PTV-based optimization and 4DRO methods. A statistically significant difference was considered when the P value was less than 0.05.

3 Results

Five lung cancer patients were evaluated for potential differences. All methods focused on RWD. This section presents key findings pertaining to these patients.

3.1 Exemplary patient

Figure 1 shows the DVH bands for the CTV and OARs derived from the 27 dose distributions for Patient 1 as an example. The results of the PTV-based optimization, RP-4DRO and EP-4DRO methods are shown in Fig. 1a–c, respectively. The dose distributions without considering the uncertainties for the reference phase (nominal scenario) are highlighted by black solid lines. For Patient 1, the bandwidths at $D_{95\%}$ for the PTV-based optimization, RP-4DRO, and EP-4DRO methods were 8.92, 8.77, and 5.29 Gy (RBE),

respectively. Correspondingly, the bandwidths at $D_{5\%}$ were 2.11, 2.11, and 1.68 Gy (RBE). The planning objective of CTV coverage was set to $D_{95\%}/D_{\text{pre}} \geq 95\%$ in the nominal scenario. The CTV coverages in the nominal scenario for the PTV-based optimization, RP-4DRO, and EP-4DRO methods were 94.86%, 93.51%, and 96.73%, respectively.

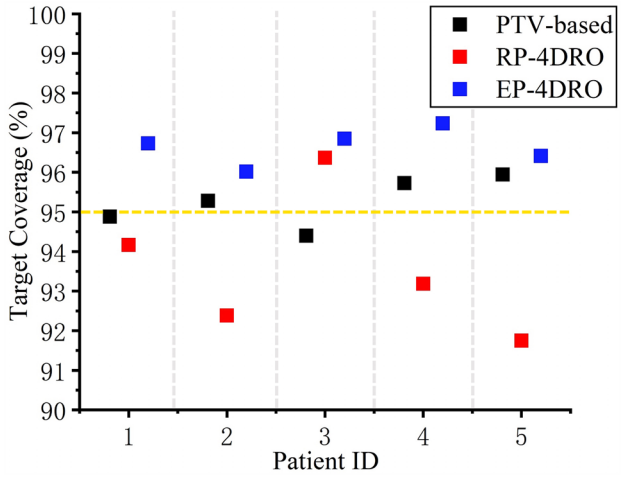

Fig. 2 (Color online) Target coverage indices for the nominal scenario

For the DVHs of the normal structures, both 4DRO methods realized narrower bands when compared to the PTV-based optimization in lung, heart, and spinal cord sparing. A nominal view of the accumulated 4D dose distributions in the reference phase for Patient 1 is presented in Fig. 1d–f. The dose at the edges of the CTV for both 4DRO methods was reduced when compared to the PTV-based optimization. Notably, the RP-4DRO method (Fig. 1e) showed hot spots in the medial area of the CTV when compared with the EP-4DRO method (Fig. 1f).

3.2 Entire patient cohort

Figure 2 shows the target coverage indices for the nominal scenario.

Compared with the PTV-based optimization, the target coverage indices realized by the RP-4DRO method were relatively low, except for Patient 3 ($P = 0.383$). The target coverage indices were also below constraint ($D_{95\%}/D_{\text{pre}} \geq 95\%$).

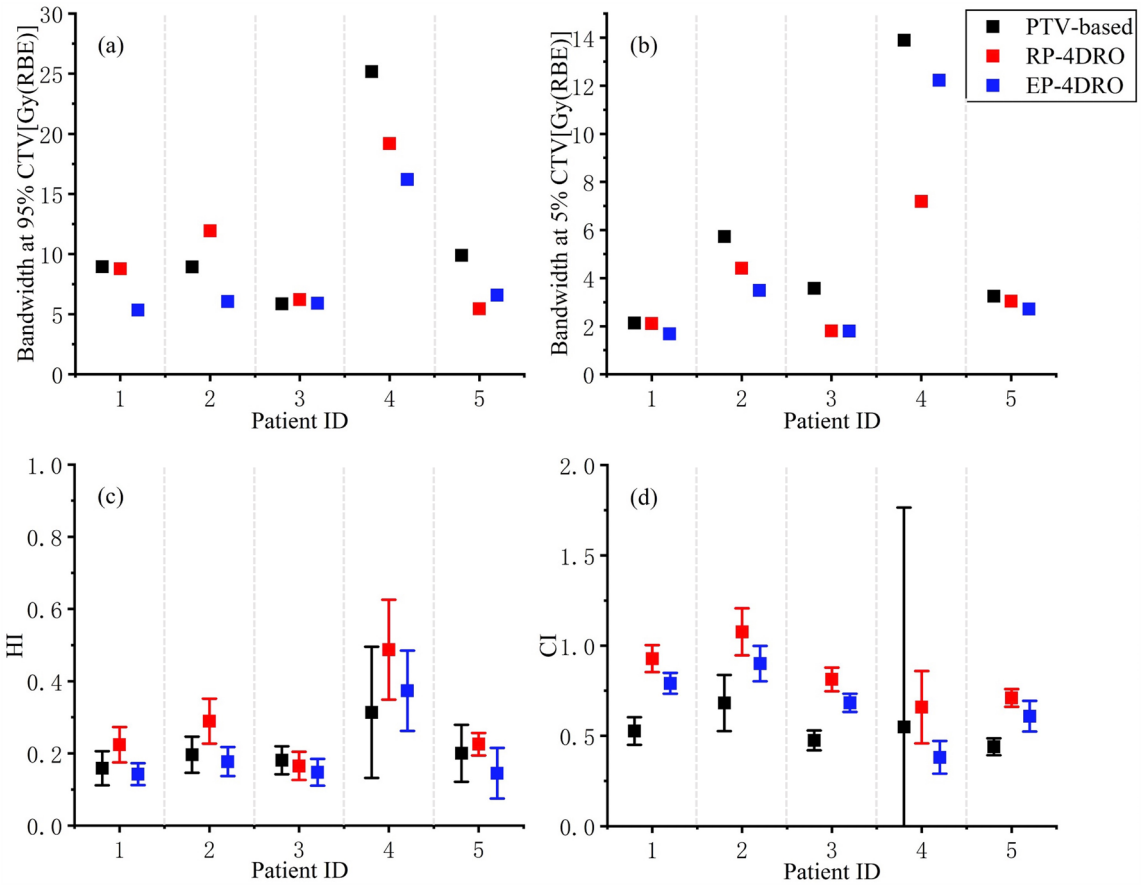

Fig. 3 (Color online) Bandwidth at 95% CTV volume (**a**) and bandwidth at 5% CTV volume (**b**) for the PTV-based optimization, RP-4DRO, and EP-4DRO approaches. The error-bar of heterogeneity (**c**) and conformity indices (**d**), respectively

Conversely, the EP-4DRO method exhibited superior performance in terms of target coverage for all patients ($P = 0.225$).

Figure 3 shows the robustness evaluation results and plan qualities with three optimization methods from five patients. The bandwidths at 95% and 5% CTV volumes for all three methods are shown in Fig. 3a, b, respectively. A lower value indicated a higher level of robustness. Based on the experimental findings, the dose distributions within the CTV derived from EP-4DRO exhibited narrower bandwidths than those achieved through PTV-based optimization, except for Patient 3. Similarly, the RP-4DRO method yielded narrower bandwidths in the dose distributions when compared to the PTV-based optimization, with the exception of Patients 2 and 3.

Figure 3c, d present the values of HI and CI for all 27 scenarios across the five patients. Error bars have been added to the figure to indicate one standard deviation of the results. For the EP-4DRO method, the HI values were generally lower than those for the RP-4DRO method and PTV-based optimization ($P = 0.345$), except for Patient 4. Lower values indicate better dose homogeneity at the target boundaries. Conversely, the RP-4DRO method yielded relatively higher HI values, indicating worse dose homogeneity in the individual respiration phases ($P = 0.107$). As shown in Fig. 3d, the CI values obtained using the EP-4DRO method are higher compared to the PTV-based optimization ($P = 0.160$) and RP-4DRO method. The CI values produced by the EP-4DRO method were higher than those of the PTV-based optimization except for Patient 4 ($P = 0.005$).

As shown in Fig. 4, the dose-volume indices for the OARs are also calculated. A comparative analysis revealed that the RP-4DRO method delivered lower doses to the lung ((left/right) lung D_{mean}, $P < 0.05$; left lung $V20$, $P = 0.068$; (left/right) lung $V5$, $P < 0.05$; and right lung $V20$, $P < 0.05$). As shown in Fig. 5, both 4DRO methods yielded lower indices for the heart and spinal cord when compared to the PTV-based optimization ($P < 0.05$), indicating the heart and spinal cord received less doses. Notably, for the five patients, the RP-4DRO method consistently exhibited the lowest doses to the lungs and heart across the individual breathing phases. However, the RP-4DRO method did not demonstrate superiority in maintaining lower doses delivered to the spinal cord when compared with the EP-4DRO method. The P values indicate that the differences in the OARs indices between the two 4DRO methods were statistically significant.

The aforementioned results illustrate 27 dose distributions for the three respiratory phases. However, for further analysis in a clinical implementation, it is necessary to compare and calculate the accumulated dose distributions over the three respiratory phases.

The bandwidth at 95% CTV volume and target coverage of the cumulative distributions are shown in Fig. 6. The RP-4DRO method showed a smaller bandwidth at 95% CTV volume when compared to the PTV-based optimization ($P = 0.022$). Conversely, the EP-4DRO method does not guarantee small bandwidths for Patient 2 and Patient 5 when compared with the PTV-based optimization ($P = 0.272$). The target coverages generated by the RP-4DRO method ($P = 0.45$) and EP-4DRO method ($P = 0.066$) were lower than that of the PTV-based optimization. The dose distributions in OARs are illustrated in Fig. 7. Compared with the PTV-based optimization, both 4DRO methods achieved lower doses in the lung, heart, and spinal cord ($P < 0.05$). Notably, the EP-4DRO method resulted in the lowest doses in the lungs and heart. In contrast, the EP-4DRO method was not superior in maintaining the lowest cumulative dose distribution delivered to the spinal cord. This implied that the accumulated dose distributions generated by both 4DRO methods are more conservative.

4 Discussion

Both 4DRO methods have been proposed to improve the robustness of treatment plans for carbon-ion IMPT. Although many studies have investigated the responses of patients with diverse cancers to various optimization methods, there have been no direct comparisons between the RP-4DRO and EP-4DRO methods. Consequently, this study aimed to systematically compare and evaluate both 4DRO methods in carbon-ion IMPT treatment planning.

The EP-4DRO method can ensure plan robustness in individual respiratory phases, as shown in Fig. 3a, b. Conversely, the RP-4DRO method ensures the robustness of the cumulative dose distributions, specifically in the reference respiratory phase, as illustrated in Fig. 6a. This is because the RP-4DRO method does not explicitly optimize the dose distributions of individual breathing phase.

Regarding target heterogeneity (Fig. 3c, d), the EP-4DRO method shows superior dose homogeneity inside the target boundaries when compared to the PTV-based optimization and RP-4DRO methods. Both 4DRO methods outperformed in the dose distribution conformity when compared to the PTV-based optimization except for Patient 4. This discrepancy can be attributed to the inherent challenge of ensuring dose-distribution conformity for smaller target movements during the optimization process.

It is vital to guarantee the target coverage for carbon-ion IMPT treatment planning. Regarding the target coverage indices in the individual respiratory phases, the EP-4DRO method ensured the target coverage. Conversely, the RP-4DRO method sacrificed the target coverage, except for Patient 3. As shown in Fig. 6b, both 4DRO methods

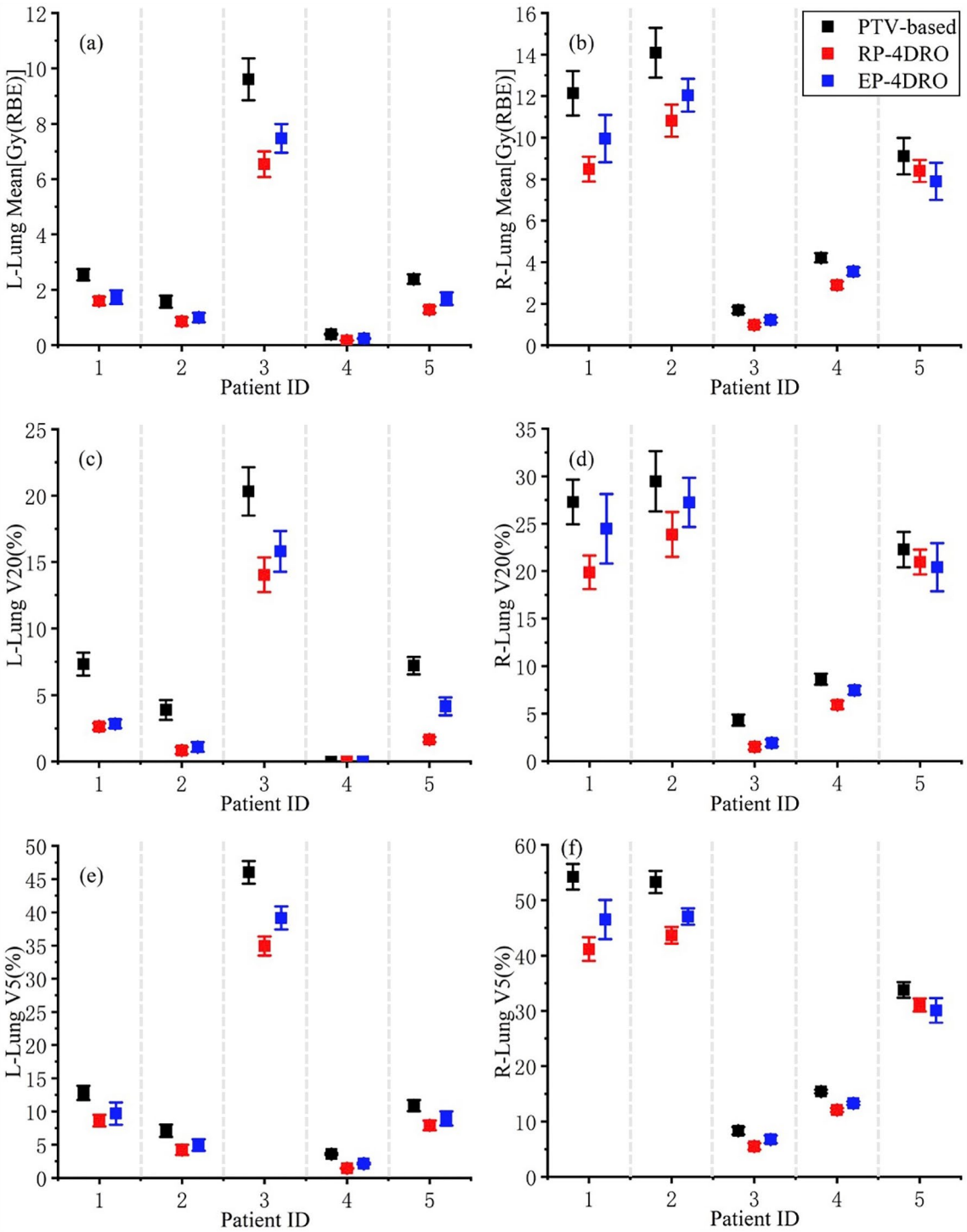

Fig. 4 (Color online) Dose distributions in lung for the PTV-based optimization, RP-4DRO, and EP-4DRO methods

sacrificed the target coverage in the reference respiratory phase. Notably, the target coverage remained unsatisfactory for the uncertainty scenarios, as shown in Fig. 1. Furthermore, the target coverage achieved by the EP-4DRO method in the individual respiratory phases differed from that observed in the reference phase. This might be due to the accuracy of data processing such as deformable image registration.

Both 4DRO methods demonstrate superior OARs sparing when compared with the PTV-based optimization, as indicated in Figs. 4, 5, and 7. An important finding demonstrated that the RP-4DRO method exhibited superior performance

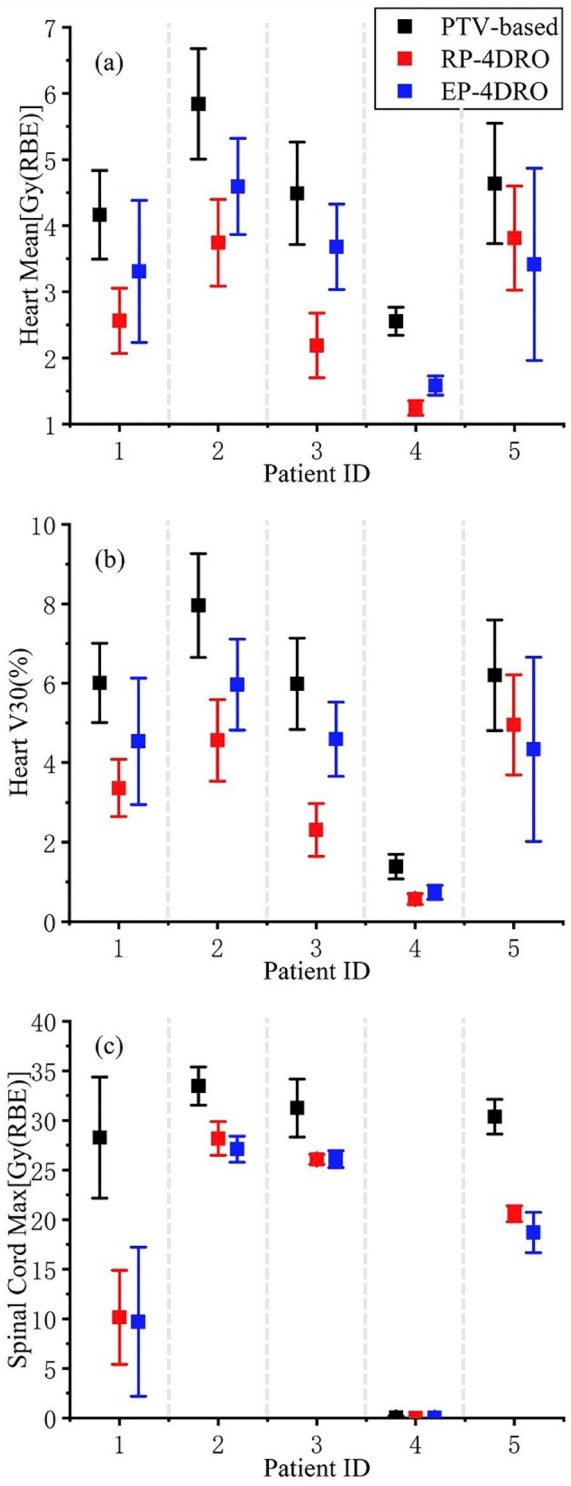

Fig. 5 (Color online) Dose distributions in heart and spinal cord for the PTV-based optimization, RP-4DRO, and EP-4DRO methods

to the EP-4DRO method in protecting the lungs and heart in both the individual respiratory phase and reference respiratory phase. However, the RP-4DRO method did not exhibit any advantage over the EP-4DRO method in terms of spinal-cord sparing. The P-values indicate that the differences in OARs indices between the two methods were statistically significant.

Generally, both 4DRO methods yielded different results because of the different dose distributions selected during the optimization process. Ge et al. [3] demonstrated that the EP-4DRO method maintained robustness even if the patient did not breathe consistently, fraction-by-fraction, over the treatment course. Our study suggests that carbon-ion IMPT treatment planning using the EP-4DRO method is superior to the RP-4DRO method in terms of robustness and planning quality while being flexible. The RP-4DRO method exhibited superior OARs protection. Thus, if we focus on OAR sparing, then the RP-4DRO method should be used. Conversely, if robustness is a priority, then the EP-4DRP method should be chosen. Furthermore, the results highlight that carbon-ion IMPT treatment planning with both 4DRO methods lead to worse target coverage for a small target volume, as observed in Patient 4. Therefore, caution should be exercised when utilizing both 4DRO methods for small-volume tumors. In comparison to proton treatment planning, the main distinction in 4D robust optimization is the optimization of the RBE-weighted dose distributions with variable RBE values. The application of 4D robust optimization methods to carbon-ion treatment planning should be further investigated.

It is crucial to recognize the inherent limitations of this study. These five patients with lung cancer may not provide a comprehensive representation of all cases of lung cancer. In future investigations, it is imperative to carefully consider a larger cohort of patients with cancer to ensure a more inclusive analysis. Moreover, this study only included three breathing phases. The next step would involve adopting additional respiratory phases to ascertain whether similar results can be obtained. Finally, it is essential to explore the potential uncertainties associated with RBE in future research. This is significant because the RBE value plays a critical role in calculating the biological dose of carbon ions.

The interplay effect due to the interference of the dynamic beam delivery and target motion leads to the deterioration of dose distributions. The severity of the interplay effects could potentially be reduced by the favorable selection of treatment parameters such as beam direction, scan speed, and scan path. However, these strategies do not fully exclude relevant interplay effects. Bert et al. [28] expected relevant residual interplay effects even after 30 fractions. Richter et al. [29] suggested that increasing the beam spot size was an efficient motion mitigation option readily available at most scanning facilities especially for large tumors. The reduced presence of internal dose gradients decreases susceptibility to the interplay effects of robust dose distributions [7]. For a fair comparison with

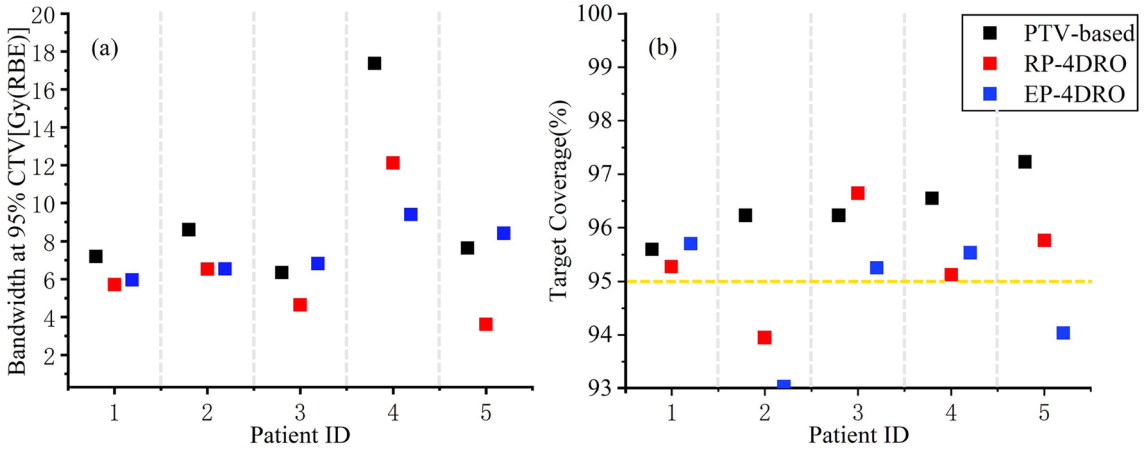

Fig. 6 (Color online) Accumulated results of robustness and target coverage for the PTV-based optimization, RP-4DRO, and EP-4DRO methods

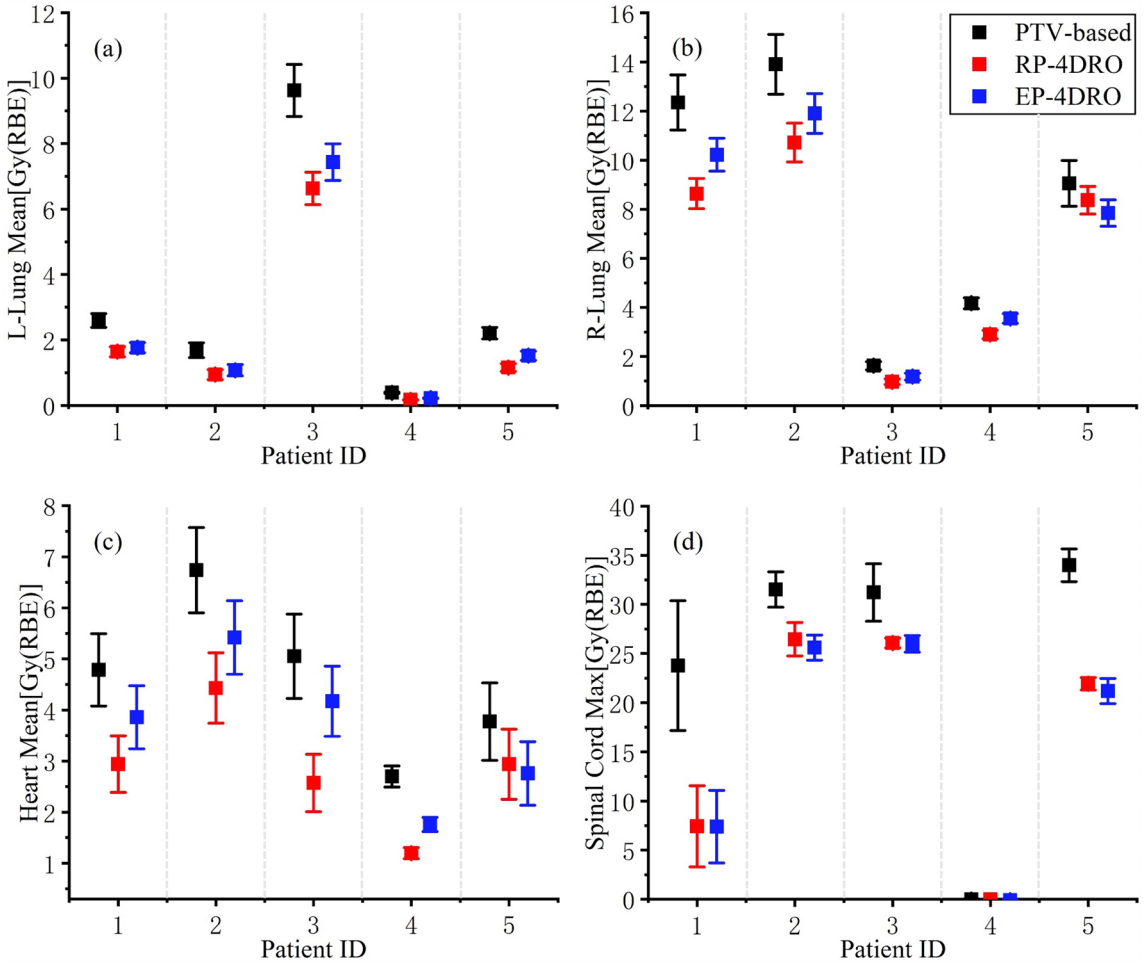

Fig. 7 (Color online) Accumulated dose distributions in lung, heart, and spinal cord for the PTV-based optimization, RP-4DRO, and EP-4DRO methods

perfectly synchronized 4D robust optimization, the interplay effect was not considered in this study. Nevertheless, efforts to further reduce the interplay effects should be differentially considered for particle therapies using different ion species.

5 Conclusion

In this study, both 4DRO approaches were implemented for carbon-ion IMPT treatment planning, which explicitly incorporated the range, setup uncertainty, and target positioning uncertainties due to breathing motion. The clinical application potential of both 4DRO methods was evaluated in five patients with lung cancer. Our results indicated that the EP-4DRO method exhibits superior robustness and plan quality, whereas the RP-4DRO method performs better in OARs sparing. Both 4DRO methods outperformed the PTV-based optimization when confronted with various uncertainties encountered during carbon-ion IMPT treatment planning.

Author Contributions All authors contributed to the study conception and design. Material preparation, data collection, and analysis were performed by Wen-Yu Wang, Yuan-Yuan Ma, Hui Zhang, Xin-Yang Zhang, Jing-Fen Yang, Xin-Guo Liu, and Qiang Li. The first draft of the manuscript was written by Wen-Yu Wang, and all authors commented on previous versions of the manuscript. All authors read and approved the final manuscript.

Data availability statement The data that support the findings of this study are openly available in Science Data Bank at 10.57760/sciencedb.j00186.00199 and https://cstr.cn/31253.11.sciencedb.j00186.00199.

Declarations

Conflict of interest The authors declare that they have no competing interests.

References

1. K. Anderle, J. Stroom, S. Vieira et al., Treatment planning with intensity modulated particle therapy for multiple targets in stage IV non-small cell lung cancer. Phys. Med. Biol. **63**, 025034 (2018). https://doi.org/10.1088/1361-6560/aa9c62
2. Y. Luo, S.C. Huang, H. Zhang et al., Assessment of the induced radioactivity in the treatment room of the heavy-ion medical machine in Wuwei using PHITS. Nucl. Sci. Tech. **34**, 29 (2023). https://doi.org/10.1007/s41365-023-01181-8
3. S. Ge, X. Wang, Z. Liao et al., Potential for improvements in robustness and optimality of intensity-modulated proton therapy for lung cancer with 4-dimensional robust optimization. Cancers **11**, 35 (2019). https://doi.org/10.3390/cancers11010035
4. A.J. Lomax, Intensity modulated proton therapy and its sensitivity to treatment uncertainties 1: the potential effects of calculational uncertainties. Phys. Med. Biol. **53**, 1027–1042 (2008). https://doi.org/10.1088/0031-9155/53/4/014
5. J. Löf, B.K. Lind, A. Brahme, An adaptive control algorithm for optimization of intensity modulated radiotherapy considering uncertainties in beam profiles, patient set-up and internal organ motion. Phys. Med. Biol. **43**, 1605–1628 (1998). https://doi.org/10.1088/0031-9155/43/6/018
6. A.J. Lomax, Intensity modulated proton therapy and its sensitivity to treatment uncertainties 2: the potential effects of inter-fraction and inter-field motions. Phys. Med. Biol. **53**, 1043–1056 (2008). https://doi.org/10.1088/0031-9155/53/4/015
7. M. Wolf, K. Anderle, M. Durante et al., Robust treatment planning with 4D intensity modulated carbon ion therapy for multiple targets in stage IV non-small cell lung cancer. Phys. Med. Biol. **65**, 215012 (2020). https://doi.org/10.1088/1361-6560/aba1a3
8. J. Unkelbach, M. Alber, M. Bangert et al., Robust radiotherapy planning. Phys. Med. Biol. **63**, 22TR02 (2018). https://doi.org/10.1088/1361-6560/aae659
9. J. Unkelbach, T.C.Y. Chan, T. Bortfeld, Accounting for range uncertainties in the optimization of intensity modulated proton therapy. Phys. Med. Biol. **52**, 2755–2773 (2007). https://doi.org/10.1088/0031-9155/52/10/009
10. J. Unkelbach, T. Bortfeld, B.C. Martin et al., Reducing the sensitivity of IMPT treatment plans to setup errors and range uncertainties via probabilistic treatment planning. Med. Phys. **36**, 149–163 (2009). https://doi.org/10.1118/1.3021139
11. D. Pflugfelder, J.J. Wilkens, U. Oelfke, Worst case optimization: a method to account for uncertainties in the optimization of intensity modulated proton therapy. Phys. Med. Biol. **53**, 1689–1700 (2008). https://doi.org/10.1088/0031-9155/53/6/013
12. A. Fredriksson, A. Forsgren, B. Hårdemark, Minimax optimization for handling range and setup uncertainties in proton therapy. Med. Phys. **38**, 1672–1684 (2011). https://doi.org/10.1118/1.3556559
13. W. Liu, X. Zhang, Y. Li et al., Robust optimization of intensity modulated proton therapy. Med. Phys. **39**, 1079–1091 (2012). https://doi.org/10.1118/1.3679340
14. Y. Li, P. Niemela, L. Liao et al., Selective robust optimization: a new intensity-modulated proton therapy optimization strategy. Med. Phys. **42**, 4840–4847 (2015). https://doi.org/10.1118/1.4923171
15. V.T. Taasti, D. Hattu, F. Vaassen et al., Treatment planning and 4D robust evaluation strategy for proton therapy of lung tumors with large motion amplitude. Med. Phys. **48**, 4425–4437 (2021). https://doi.org/10.1002/mp.15067
16. A. Meijers, A.-C. Knopf, A.P.G. Crijns et al., Evaluation of interplay and organ motion effects by means of 4D dose reconstruction and accumulation. Radiother. Oncol. **150**, 268–274 (2020). https://doi.org/10.1016/j.radonc.2020.07.055
17. C.O. Ribeiro, S. Visser, E.W. Korevaar et al., Towards the clinical implementation of intensity-modulated proton therapy for thoracic indications with moderate motion: Robust optimised plan evaluation by means of patient and machine specific information. Radiother. Oncol. **157**, 210–218 (2021). https://doi.org/10.1016/j.radonc.2021.01.014
18. W. Liu, Z. Liao, S.E. Schild et al., Impact of respiratory motion on worst-case scenario optimized intensity modulated proton therapy for lung cancers. Pract. Rad. Oncol. **5**, e77–e86 (2015). https://doi.org/10.1016/j.prro.2014.08.002
19. N. Saito, C. Bert, N. Chaudhri et al., Speed and accuracy of a beam tracking system for treatment of moving targets with scanned ion beams. Phys. Med. Biol. **54**, 4849–62 (2009). https://doi.org/10.1088/0031-9155/54/16/001
20. C. Graeff, Motion mitigation in scanned ion beam therapy through 4D-optimization. Phys. Medica **30**, 570–577 (2014). https://doi.org/10.1016/j.ejmp.2014.03.011
21. L. Wei, S.E. Schild, J.Y. Chang et al., Exploratory study of 4D versus 3D robust optimization in intensity modulated proton therapy

for lung cancer. Int. J. Radiat. Oncol. **95**, 523–533 (2016). https://doi.org/10.1016/j.ijrobp.2015.11.002
22. C.P. Karger and P. Peschke, RBE and related modeling in carbon-ion therapy. Phys. Med. Biol. **63**, 01TR02 (2017). https://doi.org/10.1088/1361-6560/aa9102
23. E. Cisternas, A. Mairani, P. Ziegenhein et al., matRad - a multi-modality open source 3D treatment planning toolkit. Paper presented at Jaffray, D. (eds) World Congress on Medical Physics and Biomedical Engineering, 7-12 June 2015
24. S.C. Huang, H. Zhang, K. Bai et al., Monte Carlo study of the neutron ambient dose equivalent at the heavy ion medical machine in Wuwei. Nucl. Sci. Tech. **33**, 119 (2022). https://doi.org/10.1007/s41365-022-01093-z
25. J. Higgins, A. Bezjak, A. Hope et al., Effect of image-guidance frequency on geometric accuracy and setup margins in radiotherapy for locally advanced lung cancer. Int. J. Radiat. Oncol. **80**, 1330–1337 (2011). https://doi.org/10.1016/j.ijrobp.2010.04.006
26. F.M. Kong, T. Ritter, D.J. Quint et al., Consideration of dose limits for organs at risk of thoracic radiotherapy: Atlas for lung, proximal bronchial tree, esophagus, spinal cord, ribs, and brachial plexus. Int. J. Radiat. Oncol. **81**, 1442–1457 (2011). https://doi.org/10.1016/j.ijrobp.2010.07.1977
27. F. Wilcoxon, *Individual Comparisons by Ranking Methods* (Springer, New York, 1992)
28. C. Bert, S.O. Grözinger, E. Rietzel, Quantification of interplay effects of scanned particle beams and moving targets. Phys. Med. Biol. **53**, 2253–2265 (2008). https://doi.org/10.1088/0031-9155/53/9/003
29. D. Richter, C. Graeff, O. Jäkel et al., Residual motion mitigation in scanned carbon ion beam therapy of liver tumors using enlarged pencil beam overlap. Radiother. Oncol. **113**, 290–295 (2014). https://doi.org/10.1016/j.radonc.2014.11.020